Experimental Comparison of Slip Detection Strategies by Tactile Sensing with the BioTac® on the DLR Hand Arm System

Jens Reinecke, Alexander Dietrich, Florian Schmidt, and Maxime Chalon

DLR - German Aerospace Center

Institute of Robotics and Mechatronics

Email: jens.reinecke@dlr.de

Abstract— Dexterous manipulation of everyday objects requires a precise tactile sense. Slip detection is mandatory to overcome uncertainty and compensate for external disturbances. We compare three different approaches for detecting slip. The methods are model-based slip detection via friction cones, vibration-based detection via bandpass filtering, and a common learning algorithm. They are implemented and tested on a tendon-driven two-finger setup equipped with two tactile BioTac® sensors. Several experiments are conducted to evaluate each approach. The characteristics of the methods are discussed and compared.

I. INTRODUCTION

In order to approach the human grasping capabilities, tactile sensing is undoubtedly a major step on the way. It allows to measure contact forces, contact points, and contact directions directly. Thus, internal and external forces can be distinguished precisely. In-hand localization [1] can be significantly improved by using tactile sensor information to deal with kinematic and dynamic uncertainties. Vision systems can be supported and relieved that way. Moreover, tactile sensing allows to estimate contact surfaces and identify different materials, and it greatly improves the identification of objects. Finally, the additional sensor data can also be utilized to detect slip.

Research on slip detection has a long history: Work from 1987 can be found measuring the acoustic signal occurring during slip [2]. In [3] two algorithms are compared mainly considering the frequency domain of the center of force distribution and the frequency domain of the normal forces measured by a rubber-based tactile sensor. There is also work taking both translational and rotational motions into account [4]. Another approach is presented in [5], where several sensors (vision, joint position encoders, fingertip force/torque sensors) are fused to detect slip during rolling contact. In [6] a 6-axis force/torque sensor is used to detect slip. The authors propose a method to compute the slip using the three-sigma rule and the standard deviations of 3-axis torque. A distributed-type tactile sensor is presented in [7]. It consists of bridge elements that are capable of measuring the force in three directions. One can evaluate the pressure distribution, which can be used to compute the center of pressure (COP) and to detect slip. In [8] a COP sensor is presented. The dropping force in the beginning of slip is used to adapt the grasping forces of a multi-fingered hand. Machine learning algorithms have been applied to a
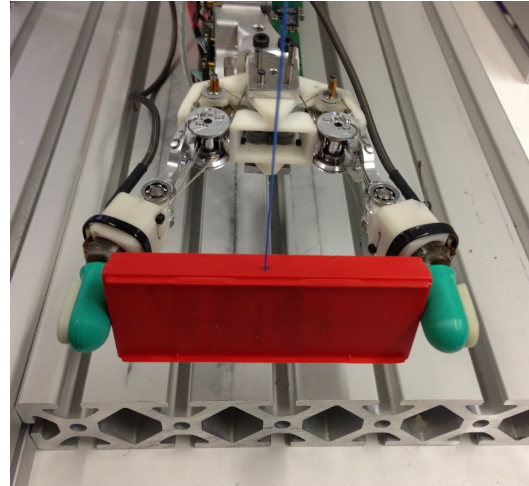

Fig. 1: Two-finger setup with BioTac® sensors

tactile sensor for detecting slip in [9]. Recent approaches [10], [11], [12] develop artificial skins to detect slip. In [10], [12] methods are proposed to analyse the frequencies which are measured by flexible conductive wires in a flexible material. There are multiple ways of detecting slippage, e. g. via COP motion, acoustic signals, sensor fusion, or frequency analyses.

The main contribution of this paper is the experimental evaluation, comparison, and discussion of three different slip detection methods: a model-based slip detection via friction cones, a vibration-based detection via bandpass filtering, and a common learning algorithm. These three methods have been chosen to compare approaches based on completely different physical principles. The friction cone approach is an intuitive way to detect slip by taking the estimated contact forces and materials into account. Applying knowledge about vibrations encountered during slip implies using frequency information instead of contact force and contact direction. The third approach, i. e. the learning algorithm, employs all available sensory information to determine slip by generating decision trees based on abtract, mathematical algorithms. Hence, apart from handing over the (nonprocessed) sensor signals and the ground truth about slip occurence during a training phase in advance, the user is not involved in terms of any further knowledge or modeling. Each of the three

methods has already been applied in the context of slip detection. To the best of our knowledge a direct comparison has not been performed so far. For the experimental evaluation, two opposing fingers of the DLR Hand Arm System [13] are equipped with BioTac® tactile sensors. Several characteristics of the detection concepts are investigated to meet the requirements of a proper comparison. These are slip detection quality, robustness against impacts, and robustness against disturbances induced by robot motions.

The organization is as follows: After a brief introduction to our test setup in Sec. II, the slip detection methods are introduced and explained in Sec. III. They are experimentally evaluated in Sec. IV and extensively discussed and compared in Sec. V.

II. Test Setup

For the experimental validation of the slip measurement approaches, we use a two-finger setup with two BioTac® sensors to reduce the complexity. This section describes the main components of the test setup, namely the fingers, the BioTac® sensors, and the software.

A. Two-Finger Setup extracted from the DLR Hand Arm System

The DLR Hand Arm System [13] is the initial step towards a new humanoid robot which can be operated safely and robustly in dynamic environments. Its Awiwi[1] hand [14] is an anthropomorphic, tendon-driven mechanism with 19 DOF (degrees of freedom). Motions are realized by 38 antagonistically arranged motors in the forearm. Additional spring elements on each tendon in the forearm lead to a high degree of mechanical robustness of the system. The sensors are shielded from impacts by placing them after these springs. This design choice also results in a more compact hand structure because most of the large mechanical and electronic components (motors, sensors, power electronics, gear boxes, communication) are outsourced into the forearm. Joint torques are computed via the tendon forces in the forearm [15]. The link side positions are model-based computed from the motor position. However, the torque measurement quality is impaired by the tendon guiding friction. Both types of guiding used (bearings and sliding) inject friction into the system. Hence, the lack of link side sensing results in degraded grasping performance because uncertainties cannot be observed precisely, and the dissipating effects are not easily identifiable.

To create a practical setup, the Awiwi hand is simplified in preparation for the experiments. An adapter is designed to hold two fingers and guide their tendons to the motors in the forearm. It is 3D printed with a simple PLA[2] polymer. The two fingers have low friction due to bearings in each joint and bearings for guiding the tendons over the joints. To use the BioTac® sensors with the Awiwi hand finger, the DIP
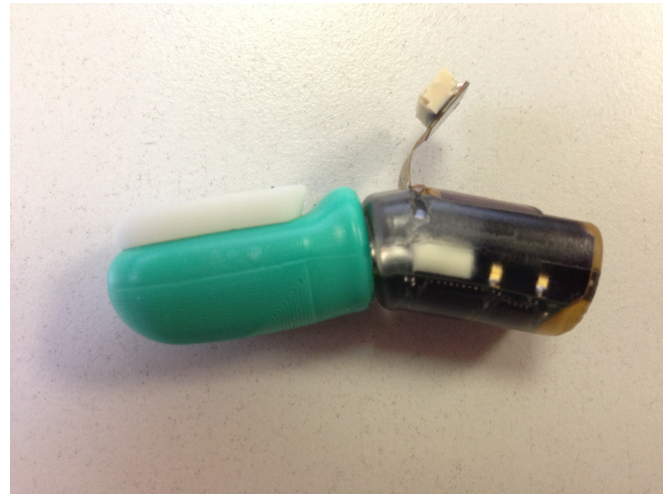
Fig. 2: BioTac® sensor

joint is removed and the PIP bone is replaced by an adapter to hold the BioTac® sensor.

B. BioTac®

The BioTac® has been developed since 2006. It uses three different measurement principles. 19 electrodes receive signals from four emitters measuring the impedance in the fluid between skin and bone surface. Their spatial distribution is restricted to the lower and front part of the finger tip. The electrodes can measure up to 12 bit impedance enabling the user to compute the contact position and direction by a weighted sum. The signals from the fast pressure sensors are processed by the inner electronics and output a slow and filtered pressure value, which is very precise ([16], p. 121). The raw pressure values obtained at 4.5 kHz can be used to measure vibrations which can be identified by a Fast Fourier Transformation (FFT), for example. Finally the third sensor type is a thermistor, providing temperature information of the touched surface supporting the material identification capabilities.

C. Software setup

The BioTac® sensors cannot be directly integrated into the forearm electronics. Therefore, they are connected to a BeagleBoard, which organizes the SPI communication and configures the sensor reading on the internal electronics. A configuration file can be assigned to the BeagleBoard to change acquisition sequence and the reading timing [17]. The BioTac® data is provided to the real time machine via UDP (User Datagram Protocol) port, which runs the two-finger setup software. This software is programmed in Simulink and compiled to C code. To view the results a viewer was programmed showing the contact point, contact force, finger configuration, and the resultant of the measured forces of the BioTac® sensors, see Fig. 3 and the attached video.

III. Slip Detection

In this section, we introduce three slip detection methods which are based on fundamentally different approaches. The
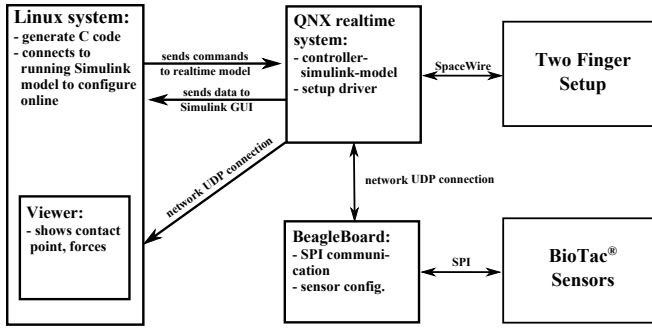
Fig. 3: Software setup with communication

Fig. 4: Friction cone shown in the contact point plane, where N describes the normal force, $\boldsymbol{F}_\mathrm{f}$ the friction force, and $\boldsymbol{F}_\mathrm{c}$ the contact force

friction cone approach in Sec. III-A utilizes a friction model to estimate the actual contact state, the bandwidth filter in Sec. III-B considers the frequencies emerging from slipping surfaces, and Sec. III-C applies a common learning algorithm that uses experience about slip gained in advance.

A. Friction Cone

1) Principle Description: If the contact force stays inside the friction cone, the grasp is known to be stable. Modern tactile sensors provide sufficient sensory information to determine contact points, forces, and directions. The angle γ is spanned between the estimated contact normal (based on the geometry of the fingertip) and the measured force direction. The direct relation to the material-combination dependent friction coefficient μ is

$$\mu = \tan\left(\gamma_0\right) . \tag{1}$$

The borders of the friction cone are described by the maximum allowed angle γ_0. The slippage is detected if the contact force is leaving the cone, that is $\gamma \geq \gamma_0$.

2) Processing: The cone axis describes the nominal contact normal. According to [18], the BioTac® sensor can be seen as half of a cylinder with a quarter sphere at the end. In order to find the contact normal to the contact point on the cylinder, one has to distinguish between contact points on the cylinder and contact points on the spherical part of the fingertip. On the cylinder, the vector between the perpendicular of the measured contact point onto the rotational axis defines the contact normal. On the spherical part of the fingertip, the vector between sphere center point and contact point is chosen. The angle γ can be easily computed from that normal and the measured contact force, see Fig. 4. One has to keep in mind that the measured force must exceed a minimum threshold to be a reliable indicator for slip. Otherwise, noise in the force could cause γ values without contact at all. The minimum treshold depends on the material combination and the grasp performed.

B. Bandwidth Filter on the Pressure Sensor Signal

1) Principle Description: In [16] the author describes how slip can be identified in the spectral analysis of the fast pressure sensor. He proposes a method which considers the amplitudes between 30 Hz and 200 Hz in particular. This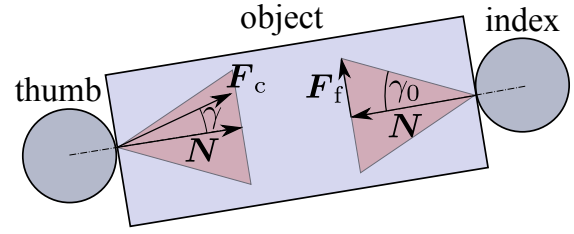 frequency range represents the vibrations during typical slippage. Interestingly, force and velocity do not influence the borders of this frequency band ([16], p. 48). An alternative detection method based on frequency analysis is proposed in [3].

2) Processing: The pressure signals of the BioTac® sensor are available at 207 Hz (slow, filtered signal) or at 4.5 kHz (unfiltered signal) [17]. The data reading of the analog digital converters is delayed by 25 μs in our configuration in order to reduce the crosstalk between the sensors. This effect is created by the capacitors in the A/D converters, which are not able to load fast enough from previous to current value. As a result, the frequency of 207 Hz is relatively low for the complete data packet. A packet contains 22 different fast pressure sensor values, which can be used to get the fast signal at 4.5 kHz. Since one packet with 22 values comes only at 207 Hz, the fast bandpass filter signal has a delay of approximately 5 ms. The obtained signal is finally bandpass filtered with the proposed band between 30–200 Hz. Afterwards, the signal is post-processed[3].

C. Learning Algorithm

1) Principle Description: Since it is not intuitive for a human to extract slip as a "binary value" from the large set of information provided by the BioTac® sensor, an automated learning algorithm is suited in this context. Such a learning algorithm can be fed with large data sets from any sensors, as long as the real slip case is additionally given to the algorithm. The ground truth must be either manually given or be obtained with the help of an extra sensor. In the present case, the pulling speed of the object is used. After the training phase, the algorithm can be used to detect slip based on the input data.

2) Processing: For the learning algorithm the open source python library Scikit-learn [19] was chosen and the random forest classifier was selected in particular. A forest of randomized decision trees is created on a set of data collected over 80 ms. The default settings of the Scikit-learn algorithm were used with 200 estimators. The forest classifiers require two arrays: one training set which contains in our case 750 samples and the truth about the slip of every sample. One sample contains 8160 features, which are all 34 different sensor values (see Table I) collected 240 times (time window

---

[3]A PT1 element is applied to the absolute values of the filtered signal.

TABLE I: Available signals in the two finger setup per finger

Signal	Description	Size	f [kHz]
motor position	incremental encoder in the motor	6	3
tendon force	tendon forces measured by the hall sensors in the spring elements in the forearm	6	3
BioTac® electrodes	measured impedance from the electrodes BioTac®	19	0.2
BioTac® thermistor	temperature from BioTac®	1	0.2
BioTac® pressure filtered	fluid pressure in the BioTac® sensor, filtered for a smooth signal	1	0.2
BioTac® pressure unfiltered	fluid pressure measured very fast for frequency analysis	1	4.5

TABLE II: Hypothesis and Experiments

Exp.	Short Description	Section
I	Pulling in x-direction	Sec. IV-A
II	Pulling in y-direction	Sec. IV-A
III	Disturbance by impact	Sec. IV-B
IV	Disturbance by motion	Sec. IV-C

of 80 ms at 3 kHz). Half of the 750 samples is used for learning and the other half for validation. The difficulty in this approach is to teach all possible cases such that the algorithm does not learn specific cases but the generic identification of slip. It may happen that the algorithm finds a simple COP motion, but if the fed cases are well selected, the algorithm can extract relationships that are too complex for humans to notice. Parameters for the algorithms are the combination of sensor input, measurement window size, the number of tree estimators, and the maximum features created when splitting a node in the tree. Increasing the number of estimators improves the quality of the learned signal, since the overfitting is decreased. However, it increases the computation time. Notice that the quality also saturates w. r. t. the number of estimators. Available signals from the test setup are shown in Table I. The forest was created offline in a training program. It can be saved and loaded to process the sensor signals online.

IV. Evaluation

In this section the three approaches are tested in multiple experiments, see Table II. The first two experiments (Sec. IV-A) investigate the slip detection at constant slip velocity. The third experiment (Sec. IV-B) investigates external impacts on the table or ground (such as footsteps) and the fourth considers oscillations or peaks induced by the robot gears and motors (Sec. IV-C). In the last section the video attachment is described, which shows that a grasp-enhancing controller employing the three signals achieves a good performance.

A. Detection Quality

1) Experiment Description: The goal of this experiment is to compare the slip detection quality of each approach. Therefore, the first step consists in building a ground truth. To do so, an object is attached to a stiff tendon[4] which is connected to a motor in the forearm. Thus, the object can be moved separately from the finger motors and the sensor data can be logged synchronously to the motor position. As
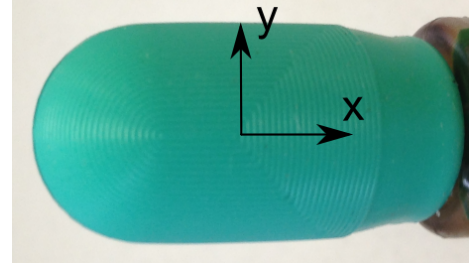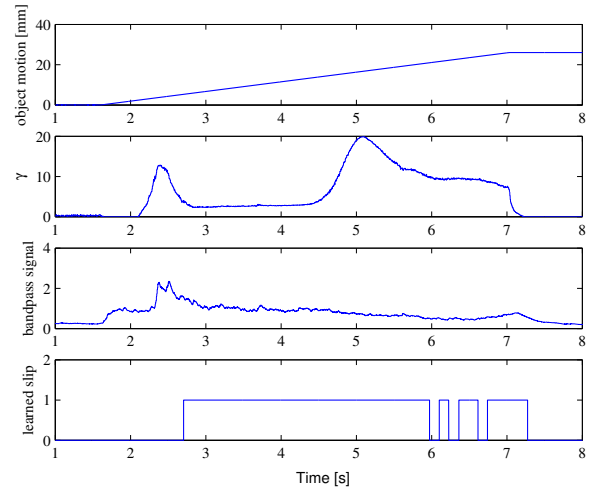
[4]The used tendon is assumed to be inelastic.

Fig. 5: Fingerprint structure of the BioTac®

Fig. 6: Detection quality in y-direction

motion profile, a ramp with constant velocity is commanded. Two pattern areas can be identified in the fingerprint with different directions as depicted in Fig. 5. The importance of having textured skin is described in [20]. The developers of the BioTac® sensor describe that the effect of the fingerprint enhances the sensed vibrations [16]. Reconfiguring the setup allows to pull the object in both directions.

2) Results: This experiment is conducted in y-direction. The object is pulled with constant velocity over a distance of 25 mm. The plots in Fig. 6 clearly show that all methods detect the slip. The learned algorithm shows a delay and some spurious errors, offering a less suitable input for a grasp-enhancing controller. The friction cone and the bandwidth approach both show peaks in the beginning due to stiction. The results of the experiment in x-direction are depicted in Fig. 7. From these measurements one can conclude that in x- and y-direction the first two approaches are more precise and faster in detecting slippage.
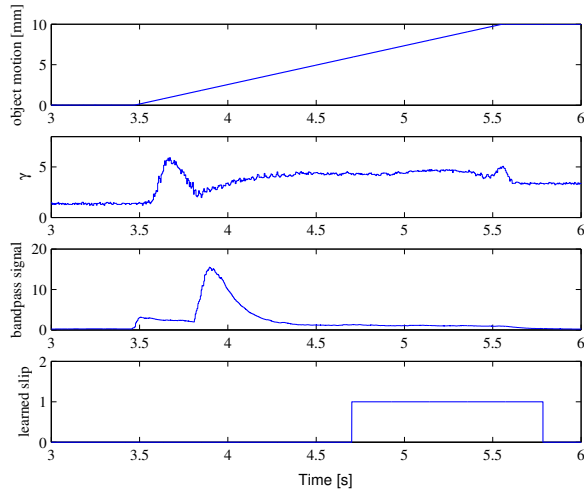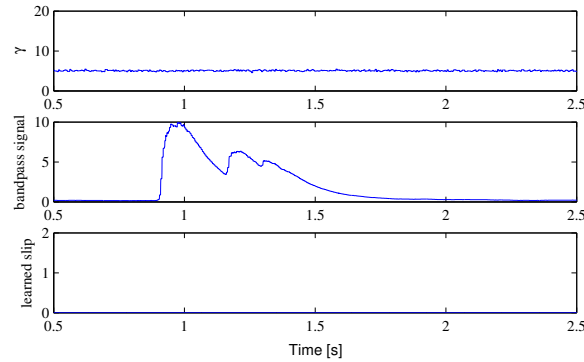
Fig. 7: Detection quality in x-direction

Fig. 8: Sensitivity to external disturbance

Fig. 9: Measurement of disturbances induced by the motion of the fingers

B. Disturbances by Impacts

1) Experiment Description: Two methods, i. e. the bandwidth filter and the learning algorithm, use the data from the fast pressure sensor which is able to measure and examine frequencies in the interesting region of 30–200 Hz, cf. Sec. II-B. This sensitivity to vibrations is also a disadvantage in terms of external disturbances from the environment. In the following, a metal ball of 0.32 kg is dropped from a height of 0.5 m onto the floor. The two-finger setup is placed on a table and the ball is dropped onto the floor next to it.

2) Results: The plot of one drop is exemplarily depicted in Fig. 8. The diagram shows that the bandwidth filter approach measures the disturbance with up to five times the amplitude of the slippage signal measured in the slippage quality experiment in Sec. IV-A. The other two methods do not feature any reaction to the ten runs.

C. Disturbances by Robot Motion

1) Experiment Description: From an application point of view it is interesting if the robot itself affects the slip detection procedure. In this experiment the test object is grasped again in the same way as in the first experiment, and the two fingers synchronously move with a sine in the abduction direction. The experiment shows if the detection is
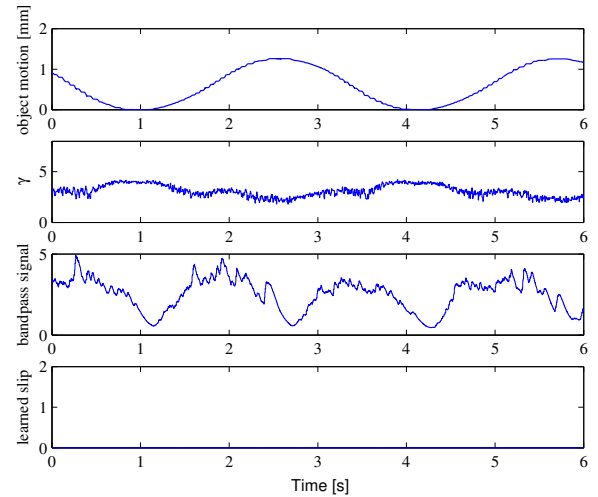
robust to internally generated noise. Among others, this noise is generated by the motors, the gear boxes, the tendons, and the controller itself.

2) Results: The results in Fig. 9 show that the parallel motion of the fingers has a small influence in the friction cone approach. This is due to a very small difference of friction in the two fingers, leading to a small difference in the amplitude of the sine motion. But it is not significantly disturbed by the motion, since the computation of the gamma depends on the electrodes, which are not sensitive to the induced frequencies. The bandpass signal shows twice the amplitude of a nominal slip signal, which might prevent the detection of slippage while manipulating an object. The learning experiment indicates no influence by the finger motion. This experiment shows that the sensitivity of the pressure sensor is really high and shows that the motors excite frequencies included in the analysed bandpass. A more damped mechanical connection between the sensor and the joints could reduce the amplitudes of internally induced frequencies.

D. Video Explanation

The controller is based on a human behavior that consists in squeezing the object if slippage is detected. In [21] an approach is shown. For the setup a simple P-controller was implemented. As input for the controller the slip detection signal from the three methods was used. The controller output is simply an addition to the joint torque to grasp more firmly. The controller is active only if a minimal grasping force is measured so as to avoid erratic behavior. The potato chip shows that the object is grasped very softly. As soon as it starts to slip the controller reacts and the potato chip crushes.

V. DISCUSSION

The experiments cover multiple characteristics of the three methods. These are summarized in Table III. The pulling

TABLE III: Slip detection approaches

Attribute	Friction cone	Bandpass filter	Learned signal
moment of detection	before and during slip	during slip	before and during slip
frequency	207Hz	3kHz	7Hz
robustness to impacts	robust	very sensitive	robust
robustness to motion	robust	sensitive	robust
direction dependency	fingerprint dependent	fingerprint dependent	fingerprint dependent
implementation difficulty	medium	easy	various learning cases needed
model	required	not required	not required
advantages(+) and drawbacks(-)	**+** robust to disturbances **+** short reaction time **−** model required for detection	**+** easy to use **+** short reaction time **−** sensitive to external disturbances **−** fast sensor required	**+** no model required **+** easy to implement **−** long training phase **−** long reaction time
possible improvements	automated threshold adjusting	vibration damped mounting for the BioTacs	use library working on a real time machine preprocess features instead of using the raw data
suitable applications	robust grasping during disturbances	fine manipulation, handling fragile objects	automated learning of complex situations

experiment showed that all methods are capable of detecting the slip in the two considered directions. The learning algorithm, however, showed a delay when detecting slip, which could be due to too few estimators in the learning algorithm. Considering detection time, the bandpass filter and the friction cone approach are superior to the learning algorithm. However, all methods have a delay of about 5 ms due to the sampling time of one BioTac® data packet. But this time span is theoretically sufficient to react to slip while grasping an object, since it can only fall about 0.12 mm freely within in 5 ms. The slow learning algorithm is not practical in a grasping force controller as we have shown in the experiments. Choosing another learning method could certainly lead to an improvement in the detection time but the general problem of the high computational effort will still remain. Regarding the quality of detection, the fingerprint is essential. All methods featured improved detection performance when the object was pulled orthogonal to the fingerprint pattern. But that also means that objects could cause problems if they only slip parallel to the fingerprint lines. The disturbance experiments showed that the bandpass signal sensitivity is disadvantageous if disturbances occur externally or internally. On the other hand this sensitivity is necessary to detect slip with small grasping forces. To increase the applicability of that method, the damping of the mechanical connection between BioTac® and robot fingers could be improved. The other two methods are robust to that kind of disturbance. Concerning the complexity of implementing the approaches, the bandpass approach is the simplest to implement, followed by the friction cone approach. The learning algorithm is rather complex since it needs a training and a predicting program for the slip signal. The variety and combination of possible input data and learning algorithm parameters offers a multiple of possibilities, but also complexity. If one does not want to deal with this high degree of complexity,

providing the algorithm with all available sensor signals has to be paid by more computational effort.

Overall, each approach is able to detect slip and each approach has clear disadvantages. The friction cone approach requires a good model of the material combination. Additionally, the Coulomb friction assumes a simple contact situation which is not present on the flexible fingertip sensor, and therefore, the threshold for detecting slip has to be adjusted for each grasp. Modeling the complex contact is not trivial and was not scope of this paper. Furthermore, a minimum force has to be applied to measure a reliable force direction, see Sec. III-A.2. The bandpass filter approach is too sensitive if the mechanical connection to the fingers is stiff, but it does not need a model of the object or the skin. Finally, the learning algorithm needs some time to be implemented and taught. It requires further implementation work to improve computation time, but it does not need a model in turn.

As shown above, the three methods have drawbacks that prevent them from being suitable in all applications. However, an elaborate fusion of the concepts could get rid of the disadvantages and benefit from the individual advantages of the concepts.

VI. CONCLUSION AND OUTLOOK

In this paper a two-finger setup with BioTac® sensors is set up and explained. Three slip detection methods were described and implemented on the test setup. An evaluation of the methods was made using real measurements in multiple experiments. The results were discussed and compared in detail, which constitutes the main contribution of this work. The comparison was summarized in a table and proposed applications for each approach. In the future the algorithms will be further augmented and fused to improve both robustness and detection quality. The learning algorithm can be reimplemented to be run on the real-time machine to increase

the frame rate. On the two-finger setup the BioTac® sensor will be used to develop and implement algorithms enabling the full Awiwi hand to grasp safer by knowing the exact state (contact points, object position, applied forces) of the object in the hand. Additionally, the BioTac® sensor values can be used to evaluate grasp quality to create a database for the robot with real measured data of grasp quality. We aim at integrating slip detection and reaction into our recently developed whole-body control frameworks and dynamic task hierarchies [22], [23].

VII. Acknowledgements

References

[1] M. Chalon, J. Reinecke, and M. Pfanne, "Online in-hand object localization," in *Proc. of the IEEE/RSJ International Conference on Intelligent Robots and Systems*, 2013, pp. 2977–2984.

[2] D. Dornfeld and C. Handy, "Slip detection using acoustic emission signal analysis," in *Proc. of the 1987 IEEE International Conference Robotics and Automation*, vol. 4, pp. 1868–1875.

[3] E. Holweg, H. Hoeve, W. Jongkind, L. Marconi, C. Melchiorri, and C. Bonivento, "Slip detection by tactile sensors: Algorithms and experimental results," in *Proc. of the 1996 IEEE International Conference on Robotics and Automation*, vol. 4, pp. 3234–3239.

[4] C. Melchiorri, "Slip detection and control using tactile and force sensors," *IEEE/ASME Transactions on Mechatronics*, vol. 5, no. 3, pp. 235–243, 2000.

[5] T. Hasegawa and K. Honda, "Detection and measurement of fingertip slip in multi-fingered precision manipulation with rolling contact," in *Proc. of the International Conference on Multisensor Fusion and Integration for Intelligent Systems*, 2001, pp. 43–48.

[6] H. Kanno, H. Nakamoto, F. Kobayashi, F. Kojima, and W. Fukui, "Slip detection using robot fingertip with 6-axis force/torque sensor," in *Robotic Intelligence In Informationally Structured Space (RiiSS), 2013 IEEE Workshop on*, April 2013, pp. 1–6.

[7] N. Tsujiuchi, T. Koizumi, A. Ito, H. Oshima, Y. Nojiri, Y. Tsuchiya, and S. Kurogi, "Slip detection with distributed-type tactile sensor," in *Proc. of the IEEE/RSJ International Conference on Intelligent Robots and Systems*. IEEE, 2004, pp. 331–336.

[8] D. Gunji, Y. Mizoguchi, S. Teshigawara, A. Ming, A. Namiki, M. Ishikawaand, and M. Shimojo, "Grasping force control of multi-fingered robot hand based on slip detection using tactile sensor," in *Proc. of the IEEE International Conference on Robotics and Automation*. IEEE, 2008, pp. 2605–2610.

[9] A. Mazid and A. Ali, "Grasping force estimation detecting slip by tactile sensor adopting machine learning techniques," in *TENCON 2008 - 2008 IEEE Region 10 Conference*, Nov 2008, pp. 1–6.

[10] M. Strohmayr, "Artificial skin in robotics: a comprehensive interface for system-environment interaction," Ph.D. dissertation, Karlsruhe, Karlsruher Institut fuÌLr Technologie (KIT), Diss., 2012, 2012.

[11] I. Fujimoto, Y. Yamada, T. Morizono, Y. Umetani, and T. Maeno, "Development of artificial finger skin to detect incipient slip for realization of static friction sensation," in *Proc. of the IEEE International Conference on Multisensor Fusion and Integration for Intelligent Systems*. IEEE, 2003, pp. 15–20.

[12] M. Vatani, E. D. Engeberg, and J.-W. Choi, "Force and slip detection with direct-write compliant tactile sensors using multi-walled carbon nanotubes/polymer composites," *Sensors and Actuators A: Physical*, 2013.

[13] M. Grebenstein, A. Albu-Schäffer, T. Bahls, M. Chalon, O. Eiberger, W. Friedl, R. Gruber, U. Hagn, R. Haslinger, H. Höppner, S. Jörg, M. Nickl, A. Nothhelfer, F. Petit, J. Reill, N. Seitz, T. Wimböck, S. Wolf, T. Wüsthoff, and G. Hirzinger, "The DLR Hand Arm System," in *Proc. of the IEEE International Conference on Robotics and Automation*, 2011, pp. 3175–3182.

[14] M. Grebenstein, "Approaching human performance: The functionality driven awiwi robot hand," Ph.D. dissertation, ETH, 2012.

[15] W. Friedl, J. Reinecke, M. Chalon, and G. Hirzinger, "FAS A Flexible Antagonistic Spring element for a high performance tendon driven hand," in *Proc. of the IEEE/RSJ International Conference on Intelligent Robots and Systems*, 2011, pp. 1366–1372.

[16] J. A. Fishel, "Design and use of a biomimetic tactile microvibration sensor with human-like sensitivity and its application in texture discrimination using bayesian exploration," Ph.D. dissertation, 2012.

[17] G. L. Jeremy Fishel and G. Loeb, *Biotac Product Manual*, SynTouch LLC, February 2013.

[18] F. J. L. G. Lin, C.H., "Estimating point of contact, force and torque in a biomimetic tactile sensor," Tech. Rep.

[19] F. Pedregosa, G. Varoquaux, A. Gramfort, V. Michel, B. Thirion, O. Grisel, M. Blondel, P. Prettenhofer, R. Weiss, V. Dubourg, J. Vanderplas, A. Passos, D. Cournapeau, M. Brucher, M. Perrot, and E. Duchesnay, "Scikit-learn: Machine learning in Python," *Journal of Machine Learning Research*, vol. 12, pp. 2825–2830, 2011.

[20] M. Cutkosky, J. Jourdain, and P. Wright, "Skin materials for robotic fingers," in *Robotics and Automation. Proceedings. 1987 IEEE International Conference on*, vol. 4, Mar 1987, pp. 1649–1654.

[21] T. Takahashi, T. Tsuboi, T. Kishida, Y. Kawanami, S. Shimizu, M. Iribe, T. Fukushima, and T. Fujita, "Adaptive grasping by multi fingered hand with tactile sensor based on robust force and position control," in *Proc. of the IEEE International Conference on Robotics and Automation*, 2008, pp. 264–271.

[22] A. Dietrich, T. Wimböck, A. Albu-Schäffer, and G. Hirzinger, "Reactive Whole-Body Control: Dynamic Mobile Manipulation Using a Large Number of Actuated Degrees of Freedom," *IEEE Robotics & Automation Magazine*, vol. 19, no. 2, pp. 20–33, June 2012.

[23] A. Dietrich, C. Ott, and A. Albu-Schäffer, "Multi-Objective Compliance Control of Redundant Manipulators: Hierarchy, Control, and Stability," in *Proc. of the 2013 IEEE/RSJ International Conference on Intelligent Robots and Systems*, November 2013, pp. 3043–3050.